

Excitation energies in ^{22}Mg from the $^{25}\text{Mg}(^3\text{He}, ^6\text{He})^{22}\text{Mg}$ reactionJ. A. Caggiano,^{1,*} W. Bradfield-Smith,^{2,†} J. P. Greene,¹ R. Lewis,² P. D. Parker,² K. E. Rehm,¹ and D. W. Visser²¹Physics Division, Argonne National Laboratory, Argonne, Illinois 60439²Wright Nuclear Structure Laboratory, Yale University, New Haven, Connecticut 06520

(Received 19 March 2002; published 19 July 2002)

A high-precision measurement of excitation energies in ^{22}Mg was performed using the $^{25}\text{Mg}(^3\text{He}, ^6\text{He})^{22}\text{Mg}$ reaction as a different approach to study this proton-rich, astrophysically interesting nucleus. The reaction was studied at 51.0 MeV with the Enge split-pole spectrograph at Yale. Proton-unbound states at 6.051(4) and 6.329(6) MeV were observed, confirming a recent identification of these new states with the $^{24}\text{Mg}(p,t)^{22}\text{Mg}$ reaction. There is no evidence in our data of a previously reported state at 5.837 MeV.

DOI: 10.1103/PhysRevC.66.015804

PACS number(s): 25.55.Hp, 26.50.+x, 27.30.+t

I. INTRODUCTION

Nova outbursts are explosive hydrogen burning events that occur at a rate of approximately 25 outbursts per year in our galaxy [1]. These outbursts typically occur in close binary systems in which a giant star orbits about a much more compact white dwarf. The high gravity of the white dwarf draws material, consisting of mostly hydrogen, from the giant onto the surface of the white dwarf. Once a critical temperature and density is reached, a series of proton captures, and subsequent β decays, is initiated with the heavier seed nuclei at the base of the accreted layer [2]. The exothermic reactions lead to a hotter environment and a situation of thermonuclear runaway. The subsequent explosion ejects newly created nuclei into the interstellar medium with enough velocity to escape the gravitational field of the binary system.

Nucleosynthesis and energy production rates in these explosive hydrogen burning events are poorly understood beyond the hot carbon-nitrogen-oxygen cycle. The uncertainties are tied to both the hydrodynamical and the nuclear uncertainties of the event. Since the rp process is driven by proton capture on proton-rich, unstable nuclei with short half-lives, there is little experimental information about the relevant cross sections or reaction rates. Reaction network calculations require knowledge of hundreds of reaction rates that have never been measured. These network calculations must then use nuclear information obtained through theoretical estimates, and the subsequent reaction rates are potentially uncertain by orders of magnitude. Consequently, there have been many recent experiments aimed at reducing these uncertainties to tolerable levels by using a variety of direct and indirect techniques [3].

Measurements of the energies and intensities of the γ rays emitted in the decay of any radioactive isotopes in the ejecta resulting from these events provide a powerful way to study the temperatures and densities in these explosions. However, in order to extract this information, such studies require complementary knowledge of the relevant nuclear reaction

rates as well as the development of accurate nova model codes. In this paper we address the issue of rates for the $^{21}\text{Na}(p,\gamma)^{22}\text{Mg}$ reaction that is a key [4] to understand the production of ^{22}Na in nova explosions.

It has recently been reported that Comptel/CGRO was able to detect the 1.275-MeV γ ray from ^{22}Na , but it has not yet been possible to associate this γ -ray line with a *specific* nova event [5]. This situation is expected to change with the launch of INTEGRAL [6]. ^{22}Na is thought to be produced primarily by the $^{20}\text{Ne}(p,\gamma)^{21}\text{Na}(p,\gamma)^{22}\text{Mg}(\beta^+)^{22}\text{Na}$ reaction sequence. The largest remaining nuclear uncertainty in its production is the $^{21}\text{Na}(p,\gamma)^{22}\text{Mg}$ reaction rate [4] that arises from the uncertainties in the properties of the states above the proton threshold in ^{22}Mg . As a result, the structure of ^{22}Mg has recently received much attention [7,8]. The $^{21}\text{Na}(p,\gamma)^{22}\text{Mg}$ reaction is thought to proceed primarily through two resonances in ^{22}Mg , at $E_x=5.7139(12)$ and $5.837(5)$ MeV, although results from recent experiments seem to suggest that the 5.837-MeV state may not exist at all [7,8]. The uncertainty in the reaction rate does not come from the resonance-energy uncertainty, but rather from the uncertainty in the resonance strengths for proton capture through these two levels [4]. At the present time, the resonance strengths for the 5.714 (2^+) and 5.837(≤ 5) [13,14] MeV states have been deduced based on comparison to *presumed* mirror states in ^{22}Ne and are not based on direct experimental measurement of these quantities in ^{22}Mg .

Previously, ^{22}Mg was studied primarily with the (p,t) [9] and $(^3\text{He},n)$ reactions [10–12]. However, recent measurements repeating the (p,t) reaction [7] and one using an exotic reaction $^{12}\text{C}(^{16}\text{O}, ^6\text{He})$ [8] suggest that the structure of ^{22}Mg just above the proton threshold may be different than tabulated in the Endt nuclear data compilation [13,14]. Bateman *et al.* [7] measured two new states within 1 MeV of the proton threshold, $E_x=6.046(3)$ and $6.323(6)$ MeV. The Chen *et al.* [8] measurement populates the state at 6.041 MeV, but not the one at 6.323 MeV. Neither measurement populated the tabulated state at 5.837 MeV, calling into question the existence of the state. This state had been thought to be the second-most important contributor (after the 212-keV resonance at $E_x=5.714$ MeV) to the proton capture rates in the Gamow window in ONeMg nova ($T_9=0.4$), and hence its absence would make the reaction rate slower by as much

*Present address: Wright Nuclear Structure Laboratory, Yale University, New Haven, CT 06520.

†Present address: Physics Department, Queens University, Kingston, Ontario, Canada K7L 3N6.

as a factor of 2–3. For higher temperatures, the capture reaction rate would then be dominated by either the direct capture to the ground state or capture into the 5.965-MeV level or the 6.046-MeV level seen in the Bateman *et al.* and Chen *et al.* measurements.

Consideration of spin-parity arguments is useful. The 5.837-MeV state is listed as having a spin of ≤ 5 in Ref. [13], and in the energy region of 5.35–5.95 MeV in ^{22}Ne , the possible mirror states are $J^\pi = 2^+, 3^+, 3^-,$ and 4^+ . A recent paper [15] suggests that the 5.837-MeV state might be the (natural parity) 3^- mirror of a state in ^{22}Ne . If this state has natural parity, it should be strongly populated with the (p,t) reaction, but was not seen in either (p,t) measurement, which seems to exclude the $2^+, 3^-$ and 4^+ (natural parity) assignments. A 3^+ state cannot be populated through a direct two-neutron cluster transfer, but may be weakly populated through a more complicated reaction mechanism, which has a much smaller cross section. However, no peak was seen at this location in either of the (p,t) measurements. The $^{12}\text{C}(^{16}\text{O}, ^6\text{He})$ reaction should also populate the state if it is a $2^+, 3^-$, or 4^+ , state but the state was not seen in this study either. The 5.837-MeV state was only seen in one $(^3\text{He}, n\gamma)$ experiment [11], but not in other $(^3\text{He}, n)$ and $(^3\text{He}, n\gamma)$ experiments [10,12]. If it exists at all, all of these experimental arguments circumstantially implicate this state as being the missing mirror of the 3^+ state in ^{22}Ne at 5.641 MeV, but this remains to be proven. The state should be populated in the $(^3\text{He}, ^6\text{He})$ reaction regardless of these possible spins and parities, and this is one of the reasons we chose this reaction.

II. EXPERIMENT

Historically, the $(^3\text{He}, ^6\text{He})$ reaction has been used on the most proton-rich stable targets to extend the reach of experimental work towards the proton dripline. In the present experiment, our idea was to take advantage of the more positive Q values associated with $(4N+1)$ targets ($Q_0 \approx -15$ MeV) compared to the dominant target contaminants ^{12}C and ^{16}O ($Q_0 = -31.6$ and -30.5 MeV, respectively) so that the $^{25}\text{Mg}(^3\text{He}, ^6\text{He})$ reaction products are easily separated from the ^6He groups resulting from reactions on these contaminants.

In order to help locate resonances for future $^{21}\text{Na}(p, \gamma)$ measurements, the $^{25}\text{Mg}(^3\text{He}, ^6\text{He})^{22}\text{Mg}$ reaction was chosen as a new approach to identify states, especially unnatural parity states that may not have been discovered yet. The nucleus ^{22}Mg has been studied with the $^{24}\text{Mg}(p,t)$, $^{20}\text{Ne}(^3\text{He}, n)$, and $^{12}\text{C}(^{16}\text{O}, ^6\text{He})$ reactions, which preferentially populate natural parity states. There are examples of this trend, such as studies of ^{18}Ne using the $^{20}\text{Ne}(p,t)$ and $^{12}\text{C}(^{12}\text{C}, ^6\text{He})$ reactions. In both of these cases, the unnatural parity state (2^-) at $E_x = 5.45$ MeV in ^{18}Ne was populated very weakly compared to the natural parity states in ^{18}Ne [16]. The tabulated level scheme and properties of ^{22}Mg are deduced directly from the (p,t) , $(^3\text{He}, n)$, and $(^3\text{He}, n\gamma)$ data only, and hence only natural parity states are tabulated. The $(^3\text{He}, ^6\text{He})$ reaction should be much less selective in this regard, populating unnatural as well as natural parity states. There are many advantages to studying this reaction with a

magnetic spectrograph. The ground state Q value is -15.5 MeV, which suggests that the cross section should be high enough to study individual states (~ 1 $\mu\text{b}/\text{sr}$) for beam energies of 50–55 MeV (well within the operating range of the Yale Tandem). As mentioned above, the $^{12}\text{C}(^3\text{He}, ^6\text{He})^9\text{C}$ and $^{16}\text{O}(^3\text{He}, ^6\text{He})^{13}\text{O}$ reactions (on inevitable target contaminants) have much more negative Q values ($Q_0 = -31.6$ MeV and $Q_0 = -30.5$ MeV, respectively). Thus, simply choosing the appropriate magnetic field in the spectrograph easily separates the ^6He groups due to these reactions, keeping them from reaching the focal plane detector.

The experiment was performed using the Enge split-pole spectrograph at the Wright Nuclear Structure Laboratory at Yale [8]. A beam of 51.0-MeV $^3\text{He}^{2+}$ ions with an intensity of 100–300 pA bombarded targets of enriched ^{25}Mg (0.4% ^{24}Mg , 99.2% ^{25}Mg , and 0.4% ^{26}Mg) (0.164 and 0.554 mg/cm²) to populate states in ^{22}Mg . The two calibration reactions, $^{27}\text{Al}(^3\text{He}, ^6\text{He})^{24}\text{Al}$ and $^{29}\text{Si}(^3\text{He}, ^6\text{He})^{26}\text{Si}$, were measured using targets of 0.125 mg/cm² aluminum and 0.17 mg/cm² $^{29}\text{SiO}_2$ on a 0.1 mg/cm² carbon backing. The magnetic rigidity of the spectrograph was chosen to bend the elastically scattered ^3He beam off the focal-plane detector that allowed states up to $E_x = 9$ MeV excitation in ^{22}Mg to be measured without interference from the elastically scattered beam. Alpha particles from the very prolific $^{25}\text{Mg}(^3\text{He}, ^4\text{He})$ reaction [$Q_0 = 13.25$ MeV, $\sigma(\Theta) \sim 10$ mb/sr at 7.5°] were easily separated from the ^6He particles in the spectrometer's focal-plane detector and provided a simultaneous monitoring of experimental conditions.

The spectrograph was set to accept a 4.8 msr solid angle bite, and data were measured with the spectrograph at 2 angle settings, 5 and 7.5 deg. The reaction has a relatively low kinematic dispersion at low angles ($dE/d\Theta = 33$ keV/deg at 7.5 deg), which is corrected by moving the focal-plane detector in the longitudinal (beam) direction.

III. EXPERIMENTAL RESULTS

The $^{25}\text{Mg}(^3\text{He}, ^6\text{He})^{22}\text{Mg}$ reaction was measured using three separate experimental configurations: (a) 7.5° , 0.554 mg/cm² ^{25}Mg target, (b) 7.5° , 0.164 mg/cm² ^{25}Mg target, and (c) 5° , 0.554 mg/cm² ^{25}Mg target. The ^6He spectra from these measurements are shown in Figs. 1(a–c), respectively. As a background check, the $^{26}\text{Mg}(^3\text{He}, ^6\text{He})^{23}\text{Mg}$ and $^{13}\text{C}(^3\text{He}, ^6\text{He})^{10}\text{C}$ reactions were measured at 7.5° and the resulting spectra are shown in Figs. 1(d) and 1(e). For calibration purposes, the $^{29}\text{Si}(^3\text{He}, ^6\text{He})^{26}\text{Si}$ and $^{27}\text{Al}(^3\text{He}, ^6\text{He})^{24}\text{Al}$ reactions were measured at 7.5° and 5° , respectively, and the resulting spectra are shown in Figs. 1(f) and 1(g).

For analysis purposes, the three ^{22}Mg spectra were combined to generate one high-statistics spectrum. A constant shift was applied to the two spectra in Figs. 1(a) and 1(c) and added to the spectrum in Fig. 1(b). That is, all the data were aligned as if they were all taken at 7.5 deg with the thinner target. This spectrum is shown in Fig. 2(a).

In addition to the statistical advantage of combining the spectra, the combined spectrum helps to identify background peaks that come from small target contaminants like ^{26}Mg

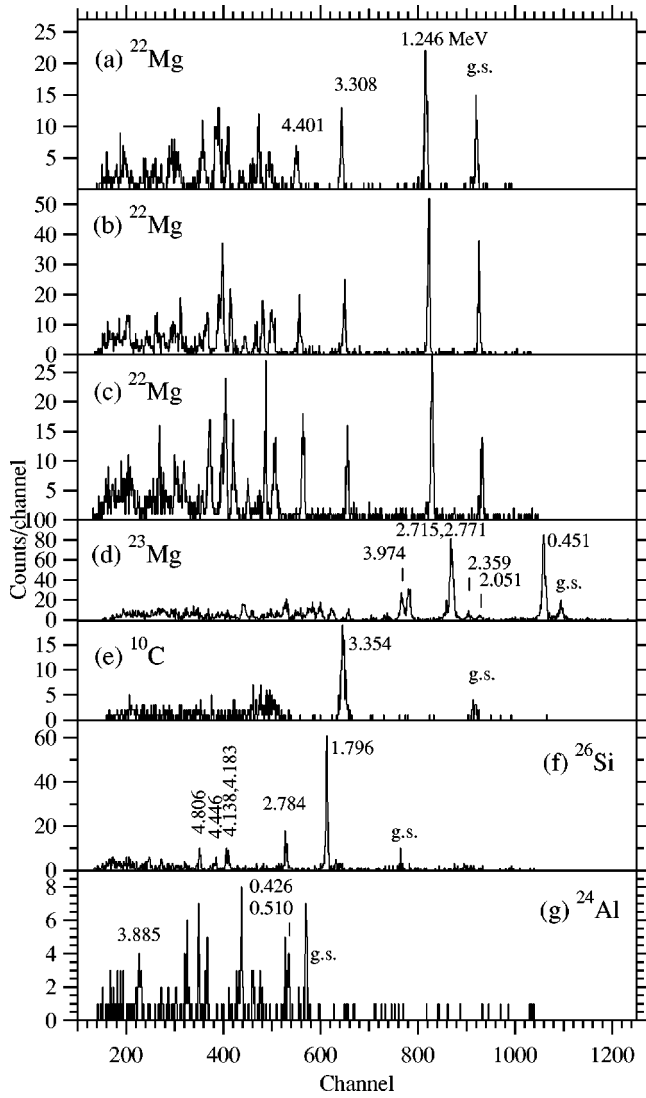


FIG. 1. All ^6He spectra taken during this experiment are from the $(^3\text{He}, ^6\text{He})$ reaction, populating states in the listed nuclei. The target and spectrograph angle settings were: (a) 0.554 mg/cm 2 ^{25}Mg target at 7.5° , (b) 0.164 mg/cm 2 ^{25}Mg target at 7.5° , (c) 0.164 mg/cm 2 ^{25}Mg target at 5° , (d) 0.396 mg/cm 2 ^{26}Mg target at 7.5° , (e) 0.1 mg/cm 2 ^{13}C target at 7.5° , (f) 0.17 mg/cm 2 $^{29}\text{SiO}_2$ target on a 0.1 mg/cm 2 carbon backing at 7.5° , and (g) 0.125 mg/cm 2 ^{27}Al target at 5° .

that may be present in the data, but are not clear in the low-statistics spectra. To deduce the contribution of the $^{26}\text{Mg}(^3\text{He}, ^6\text{He})^{23}\text{Mg}$, Fig. 2(c) shows an energy spectrum of ^6He measured with an enriched ^{26}Mg target. The excited states of ^{23}Mg at 2.715 and 2.771 MeV form the strongest peak (within the range of the ^{22}Mg spectrum), and appears in the ^{22}Mg spectrum as a peak with a height of only a few counts, indicated by the arrow in Fig. 2(a). Since the peaks from ^{23}Mg in the region of interest are much smaller, we conclude that this source of contamination is insignificant. Figure 2(b) shows a representative ^4He spectrum measured simultaneously on the ^{25}Mg target. This comparison is meant to identify any possible contamination from the pileup α events leaking into the ^6He gates. The comparison of these

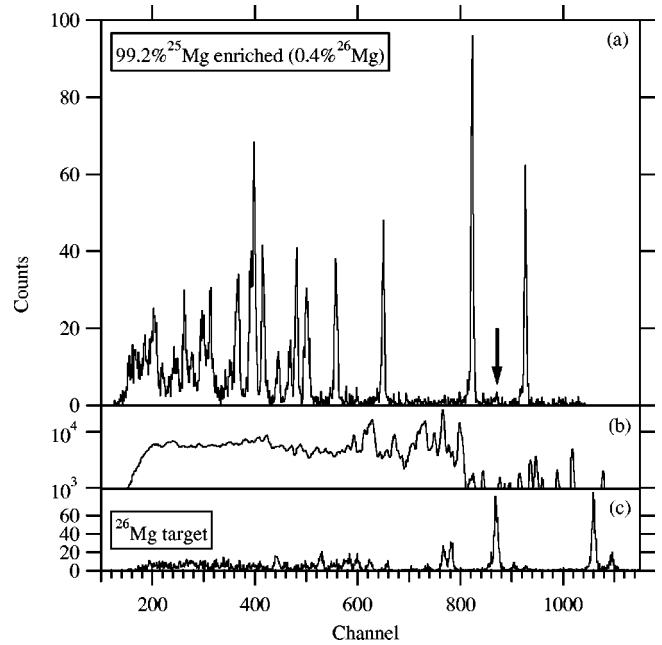


FIG. 2. (a) Energy spectrum of ^6He taken with an enriched ^{25}Mg target. (b) An α spectrum from the $(^3\text{He}, \alpha)$ reaction, measured with an ^{25}Mg enriched target. (c) Energy spectrum of ^6He measured using an enriched ^{26}Mg target. The arrow in (a) is pointing to a small peak that is the largest spectrum contamination, arising from the $^{26}\text{Mg}(^3\text{He}, ^6\text{He})^{23}\text{Mg}^*(2.715, 2.771 \text{ MeV})$ reaction on the small amount of ^{26}Mg in the ^{25}Mg targets. These figures clearly indicate that contamination is not a problem.

three figures clearly indicates that spectrum contamination from these sources is not a problem.

Many states were populated in the $^{25}\text{Mg}(^3\text{He}, ^6\text{He})^{22}\text{Mg}$ reaction [$Q_0 = -15.4589(17) \text{ MeV}$ [17]]. The ground state and well-known states at $E_x = 1.2463(6)$, 3.3082(8), 4.4009(14), and 5.7139(12) MeV from this reaction were used in the focal-plane detector calibration. Of all the states populated in the $^{29}\text{Si}(^3\text{He}, ^6\text{He})^{26}\text{Si}$ reaction [$Q_0 = -17.413(3) \text{ MeV}$ [17]], only those states that were well populated, were well isolated, and had small uncertainties were used in the calibration; these were states in ^{26}Si at 1.7959(2), 2.7835(4), and 4.806(3) MeV. The $^{27}\text{Al}(^3\text{He}, ^6\text{He})^{24}\text{Al}$ reaction [$Q_0 = -19.805(4) \text{ MeV}$ [17]] at 5° populated states in ^{24}Al at 0.0, 0.4258(1), 0.510(5), 1.107(6), 1.275(9), 1.559(13), 2.349(20), 2.534(13), 2.810(20), and 3.885(25) MeV and all were used in the calibration. The calibration was performed by using these known states to determine magnetic rigidity as a polynomial function of focal-plane position [$B\rho(x)$]. Fits up to sixth order yield the same results within a few keV, but the reduced χ -squared parameter is minimized for the linear fit. The values of the states extracted varied slightly (0–20 keV, depending on the state) with the polynomial fit order and these variances are included in the quoted error bars (see Table I).

Figure 3 shows the ^6He spectrum from $E_x = 4.0$ to 9.2 MeV with deduced excitation energies, and Table I summarizes all peaks and compares them with recent work [7,8] and the values listed in the data compilation [13,14]. Measured values and uncertainties are extracted for all states where

TABLE I. Excitation energy results presented here and elsewhere. States marked with an asterisk were used for calibration.

E_x from this work (MeV)	Endt [13,14]	Chen <i>et al.</i> [8]	Bateman <i>et al.</i> [7]	J^π (Endt [13,14])
0.0*	0.0			0^+
1.2463*	1.2463(6)			2^+
3.3082*	3.3082(8)			$(4)^+$
4.4009*	4.4009(14)	4.408(12)	4.400(4)	$(2)^+$
	5.006(2)			$(0^+ - 4^+)$
5.033(7)	5.0370(14)	5.029(12)	5.0370*	2^+
5.094(6)			5.0897(17)	
5.301(4)	5.292(3)	5.272(9)	5.2957(16)	$(2^+, 3)$
	5.317(5)			$(1-3)$
5.451(5)	5.464(5)		5.4543(16)	$(2-4)$
5.7139*	5.7139(12)	5.711(13)	5.7139*	2^+
	5.837(5)			≤ 5
	5.965(25)		5.9619(25)	0^+
6.051(4)		6.041(11)	6.046(3)	
6.246(4)	6.267(15)	6.255(10)	6.246(5)	4^+
6.329(6)			6.323(6)	4^+
6.616(4)	6.585(35)	6.606(11)	6.613(7)	
6.771(5)	6.783(19)	6.767(20)	6.787(14)	3^-
6.878(9)		6.889(10)		
	6.980(80)			3^-
7.206(6)	7.213(18)	7.169(11)		0^+
7.373(9)		7.402(13)		
7.606(11)				
7.757(11)		7.784(18)		
	7.840(90)			
7.916(16)				
7.986(16)	7.945(45)	7.964(16)		
8.229(20)		8.203(23)		
	8.290(40)			
8.394(21)		8.396(15)		
8.487(36)				
		8.547(18)		
8.598(20)		8.613(20)		
8.789(20)		8.754(15)		

there was a clear peak above background. The strong peak between the 4.4009 and 5.301 MeV peaks is clearly a doublet because of its breadth, but it is unresolved. The excitation energies extracted by fitting the peak with a doublet are 5.033(7) and 5.094(6) MeV, in excellent agreement with the doublet measured recently in Ref. [7]. The states measured at 5.301(4) and 5.451(5) MeV are also in excellent agreement with Ref. [7] and are presumed to be the 5.295 and 5.464 MeV states listed in Ref. [13]. The 5.7139-MeV state was observed and provides a good calibration point, as mentioned earlier. The state at 6.051(4) MeV measured here was first seen in a (p,t) measurement at 6.061(37) MeV [9] but, for an unknown reason, was not included in the nuclear data compilation [13,14]. The state was also observed in Refs. [8] and [7]. There is a small shoulder on the 6.051-MeV state, which may be the 5.965-MeV state, but it is too weak to allow us to draw any conclusions about it. Two states at

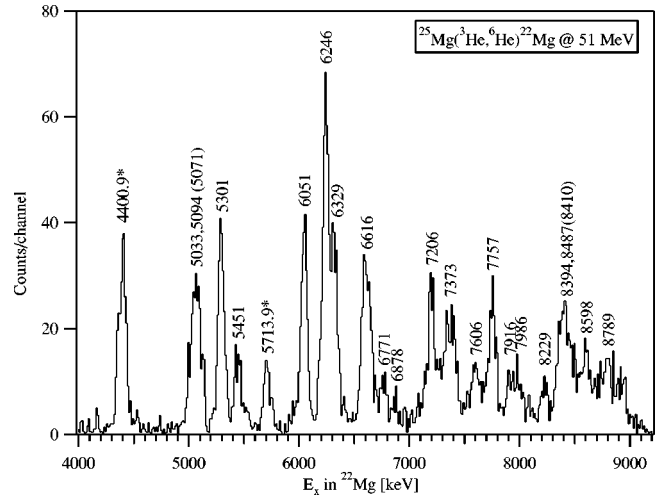


FIG. 3. Spectrum from all the $^{25}\text{Mg}(^3\text{He}, ^6\text{He})^{22}\text{Mg}$ reaction data taken in this experiment, combined and calibrated for excitation energy for ^{22}Mg . The numbers indicate the states populated. States labeled with asterisks indicate which states were used in the calibration. Broad peaks, i.e., significantly wider than spectrum resolution, are labeled with two energies (fit by a double Gaussian function) and one in parentheses (fit by a single Gaussian function).

6.246(4) and 6.329(6) MeV appear as a strong, resolved doublet in our spectrum. The state listed at 6.267 MeV in Ref. [13] is most probably some combination of these two states, which are also seen as separate states at 6.246(5) and 6.323(6) MeV in Ref. [7]. Only one of the two states is observed in Ref. [8] at 6.255 MeV. A doublet of states at 8.394 and 8.487 MeV appear as a broad, asymmetric peak indicative of a broad state. However, this is just 250 keV above the α threshold and therefore the α width must be very small (≤ 1 keV). Consequently, we chose to fit this state as a doublet.

Other states seen in this experiment are labeled in Fig. 3 and listed in Table I with their error bars. The uncertainties are dominated by statistics, but include systematic error contributions from scattering angle ($\pm 0.05^\circ$) and calculated energy losses ($\pm 5\%$). Uncertainty in the beam energy (at most 50 keV) makes only a negligible contribution (< 1 keV) since the $(^3\text{He}, ^6\text{He})$ reaction is used for the calibrations as well as the measurements. The uncertainties in the masses of ^{26}Si (3 keV), ^{22}Mg (1.4 keV), and ^{24}Al (4 keV) [17] were included in the uncertainties of the points used for calibration. An additional 11-keV uncertainty was conservatively estimated for states above $E_x = 8.0$ MeV due to extrapolation outside the range of momentum calibration, and has been added directly to their quoted error bars.

IV. DISCUSSION

The state listed in the literature at 5.837 MeV was not observed with this reaction. It was not observed in any of the (p,t) studies [7,9], nor was it measured in the $(^{16}\text{O}, ^6\text{He})$ reaction [8]. The state was seen in one $^{20}\text{Ne}(^3\text{He}, n\gamma)$ measurement [11], but not in other $^{20}\text{Ne}(^3\text{He}, n\gamma)$ studies [12,10]. This evidence suggests that the state may not exist in

^{22}Mg . The absence of the state at 5.837 ($E_r=337$ keV) reduces the reaction rate substantially by a factor of 2–3 in the nova temperature regime of $T_9=0.1-0.4$. The additional state at 6.051 MeV ($E_r=551$ keV) is above the Gamow window for ONeMg novae ($T_9=0.4$) and its contribution to these burning scenarios is therefore weak. The new state at 6.329 MeV is above the Gamow window for $T_9\leq 0.6$ and hence does not contribute in novae, but may be relevant for explosive hydrogen burning in hotter environments such as x-ray bursts or supernovae. Detailed reaction rates are included in Ref. [7] work and hence are not reproduced here.

V. SUMMARY

In order to help locate resonances for future $^{21}\text{Na}(p, \gamma)$ measurements, the $^{25}\text{Mg}(^3\text{He}, ^6\text{He})^{22}\text{Mg}$ reaction was chosen as a new approach to identify states, especially unnatural parity states, which may not have been discovered yet. States were measured in the ^{22}Mg with the never before used reac-

tion $^{25}\text{Mg}(^3\text{He}, ^6\text{He})^{22}\text{Mg}$. This new approach confirms the existence of two new states, and we measure their locations at $E_x=6.051(4)$ and $6.329(6)$ MeV. We do not find any evidence to support the existence of the 5.837-MeV state in ^{22}Mg . Many other excitation energies have been measured with high precision (0.07–0.3 %) and these measurements will reduce the overall errors in the excitation energies in ^{22}Mg . These experimental results place the structure of ^{22}Mg above the proton threshold on much firmer experimental ground. More work is needed to firmly assign spins and parities to the states observed, because recent studies still fall short of definitive assignments.

ACKNOWLEDGMENTS

This work was supported by the U.S. Department of Energy, Grant Nos. W-31-109-ENG-38 and DE-FG02-91ER-40609.

-
- [1] S. Starrfield, C. Iliadis, J.W. Truran, M. Wiescher, and W. Sparks, Nucl. Phys. **A688**, 110c (2001).
 - [2] M. Wiescher, H. Schatz, and A.E. Champagne, Philos. Trans. R. Soc. London, Ser. A **356**, 2105 (1998).
 - [3] K.E. Rehm and M.S. Smith, Annu. Rev. Nucl. Part. Sci. **51**, 91 (2001).
 - [4] J. Jose *et al.*, Astrophys. J. **520**, 347 (1999).
 - [5] A. Iyudin *et al.*, in *Proceedings of GAMMA2001: Gamma-Ray Astrophysics 2001*, edited by S. Ritz *et al.*, AIP Conf. Proc. No. 587 (AIP, Melville, NY, 2001), p. 508.
 - [6] G. Vedrenne *et al.*, Astrophys. Lett. Commun. **39**, 325 (1999).
 - [7] N. Bateman *et al.*, Phys. Rev. C **63**, 035803 (2001).
 - [8] A. Chen, R. Lewis, K.B. Swartz, D.W. Visser, and P.D. Parker, Phys. Rev. C **63**, 065807 (2001).
 - [9] R.A. Paddock, Phys. Rev. C **5**, 485 (1972).
 - [10] A.B. McDonald and E.G. Adelberger, Nucl. Phys. **A144**, 593 (1970).
 - [11] C. Rolfs *et al.*, Nucl. Phys. **A191**, 209 (1972).
 - [12] W.P. Alford *et al.*, Nucl. Phys. **A457**, 317 (1986).
 - [13] P.M. Endt, Nucl. Phys. **A521**, 1 (1990).
 - [14] P.M. Endt, Nucl. Phys. **A633**, 1 (1998).
 - [15] Nadya A. Smirnova and Alain Coc, Phys. Rev. C **62**, 045803 (2000).
 - [16] K.I. Hahn *et al.*, Phys. Rev. C **54**, 1999 (1996).
 - [17] G. Audi and A.H. Wapstra, Nucl. Phys. **A595**, 409 (1995).